JOURNAL OF EXPERIMENTAL AND THEORETICAL PHYSICS, 2024, Vol. 166, No. 4(10), pp. 441–456

ATOMS, MOLECULES, OPTICS

COHERENCE EFFECTS OF MAGNETIC SUBLEVELS INDUCED BY A LINEARLY POLARIZED WAVE FIELD IN SATURATED ABSORPTION AND MAGNETIC SCANNING SPECTRA IN ATOMS WITH Λ- AND V-TYPE TRANSITIONS

© 2024 E. G. Saprykin[a] and A. A. Chernenko[b]*

[a]*Institute of Automation and Electrometry Siberian Branch of the Russian Academy of Sciences, Novosibirsk, 630090 Russia*

[b]*Institute of Semiconductor Physics Siberian Branch of the Russian Academy of Sciences, Novosibirsk, 630090 Russia*

**e-mail: chernen@isp.nsc.ru*

Received March 12, 2024

Revised April 08, 2024

Accepted April 10, 2024

Abstract. It has been shown analytically and numerically that the effect of magnetic coherence (interference) of levels in Λ- and V-type transitions, induced by the field of a traveling linearly polarized electromagnetic (EM) wave of arbitrary intensity, can make a significant contribution both to the populations of transition levels (more $\sim 50\%$ than of the field contribution) and to the absorption resonance spectra during frequency and magnetic scanning. Differences in the manifestation of the magnetic coherence effect in level populations for open and closed types of transitions have been identified. It has been established that narrow coherent electromagnetically induced transparency (EIT) resonances are formed in the absorption resonance spectra during magnetic scanning near zero magnetic field. The dependencies of EIT resonance parameters on the characteristics of atomic transitions and EM wave intensity have been investigated. The contribution of the magnetic coherence effect of transition levels to the shape of these resonances has been revealed.

The article is presented as part of the conference proceedings "Physics of Ultracold Atoms" (PUCA-2023), Novosibirsk, December 2023.

DOI: 10.31857/S004445102410e031

1. INTRODUCTION

Studies of nonlinear spectroscopic effects in resonant interaction of light fields with degenerate atomic systems have been conducted for a long time. Interest in them is due to the variety of physical processes occurring in these systems, including atomic state interference effects leading to narrow resonant structures in the studied spectra (see [1]). It should be noted that the emergence of coherence of atomic states in two-photon transitions was first observed in experiments with incoherent radiation sources [2].

With the creation of lasers and the development of nonlinear laser spectroscopy, the field of research in nonlinear and coherent phenomena has expanded significantly. Currently, interest in the topic is maintained due to the development of new experimental techniques, including such challenging ones as cold atom studies.

Subsequently, resonances caused by the coherence of atomic states under laser excitation received the names of electromagnetically induced transparency (EIT) and electromagnetically induced absorption (EIA) resonances. Emerging from studies of nonlinear optical phenomena in the interaction of laser radiation with gaseous media, the scope of these effects has spread to many other systems with potential practical applications. However, the need for obtaining precise analytical solutions and interpretations of discovered phenomena maintained the connection with nonlinear spectroscopy of gaseous media, stimulated work in this field, including numerical simulation of experiments as a method allowing to investigate situations not always achievable in practice. Many of the previously discovered phenomena were "rediscovered" and renamed in works on EIT and EIA. This, as well as misconceptions in the interpretation of several results from those times, was addressed in the Introduction to work [3].

A striking example of coherent phenomena in degenerate transitions from the ground state of atoms are EIT resonance [4], which are based on the phenomenon of coherent population trapping (CPT) [5], as well as resonances of opposite sign – EIA resonances, first discovered in [6]. According to [7], the cause of EIA resonances was the effect of spontaneous transfer of magnetic coherence (MC)[1] of the excited state levels to the ground state, the manifestation patterns of which in saturated absorption spectroscopy were first considered in [8]. However, the EIA resonance anomalies later recorded in experiments [9, 10] were explained in terms of other processes, such as optical pumping and CPT [9], collisions [11], and not always reasonably, but giving resonance structures similar to the experiment. Nevertheless, in [12], developing the concept of [7], it was claimed that the main mechanism for the formation of EIA resonances at any closed transitions is precisely the spontaneous transfer of MC from upper state levels to lower state levels.

However, further studies have shown that in the formation of nonlinear resonance structures, including EIA resonances, both on simple and degenerate transitions (with level moment $J = 1/2, 1, 2$) other processes prove to be more important than the spontaneous transfer of MC of upper state levels. Thus, in [13] it is shown that in a two-level system, the narrow resonance structure in the field of two co-directed waves on an open transition manifests as an EIT resonance, and on a closed transition – as an EIA resonance. The cause of these structures is coherent beatings of level populations in the field of two frequencies [14, 15]. In the case of transitions with level moment $J = 1/2$, $J = 1$, according to [16–18], narrow resonance structures (EIT resonances) are formed in Λ-schemes of transition, where the main contribution comes from MC of lower state levels, while the contribution of spontaneous MC transfer from upper to lower state levels is small and appears as an addition. Moreover, on the transition with $J = 1$ the mechanism of EIT resonance formation depended on the field polarization directions: with parallel polarizations, the resonance was determined by coherent beatings of level populations, as in [13], and with orthogonal polarizations – by nonlinear interference effect (NIEF) [14]. The results of [16,17] are also valid for transitions of type $J \to J$ and $J \to J-1$ ($J > 1$), since on these transitions the spectra of nonlinear resonances are also formed in open Λ-schemes.

A different situation occurs on transitions of type $J \to J+1$ [17, 19], where due to the difference in oscillator strengths between magnetic sublevels, the nonlinear resonance spectrum is formed mainly in V-schemes of transition, formed by sublevels with maximum magnetic number M. It is in V-schemes that closed two-level transitions are realized, in which the form of narrow resonance structures radically depends on the degree of openness of the atomic transition [13]. The effect of spontaneous MC level transfer on this type of transitions does not affect the qualitative form of the narrow resonance structure. Moreover, the action of an intense probe field can change the type of narrow resonance (from EIT to EIA) [17].

Note that the main patterns of nonlinear resonance formation, including MC level effects, were obtained through resonant interaction of a two-frequency field with degenerate atomic transitions [16–18] and numerical solution of the problem, since analytical solutions for transitions with level momentum $J > 1$ are complex and difficult to analyze.

In this regard, it is of interest to consider the processes of absorption resonance formation in a single-wave field of linear polarization in simple Λ- and V-type atoms with a magnetically degenerate level structure. In these types of atoms, during resonant interaction with a linearly polarized electromagnetic (EM) wave field, the level population values are determined by contributions from the incoherent saturation process of level populations and a coherent addition due to magnetic coherence of levels induced by the

[1] In some works, the terms Zeeman coherence or low-frequency coherence are used.

linearly polarized wave field. The specifics of the considered transitions allow obtaining analytical solutions to the problem in quadratures, while numerical solutions make it possible to isolate the contribution of each process in its pure form, both in the populations of transition levels and in the form of absorption resonances during frequency and magnetic scanning. Furthermore, these results will help determine the applicability conditions of approximations used in the probe field method for atoms with more complex level structures.

2. SATURATION EFFECT OF LEVEL POPULATIONS IN Λ- AND V-TYPE TRANSITIONS BY LINEARLY POLARIZED EM-WAVE FIELD

Let us consider the problem of resonant interaction between a monochromatic linearly polarized traveling EM wave of arbitrary intensity and atoms having Λ- or V-type transitions. Such transitions occur between atomic state levels with total moments $J = 0$ and $J = 1$. It is assumed that the atomic medium is placed in a magnetic field with strength $\mathbf{H}$, which magnitude can vary, and the EM-wave propagates along the magnetic field direction. We will consider the problem in a coordinate system with the quantization z axis z along the direction of vector $\mathbf{H}$. In this coordinate system, in atoms in a linearly polarized EM field, transitions between levels with a change in the magnetic quantum number $\Delta M = \pm 1$ are allowed and processes shown in Fig. 1 are induced. Meanwhile, levels with magnetic number $M = 0$ of the state with moment $J = 1$ (not shown in Fig. 1) do not interact with the EM-field and do not affect the processes formed by the field.

When solving the problem, we proceed from the kinetic equations for the atomic density matrix in the model of relaxation constants [14, 20]. In this case, the dynamics of diagonal $\rho_{ii} = \rho_i$ and non-diagonal ρ_{ik} elements of the density matrix in the field of monochromatic EM wave is described by the following system of equations:

$$\frac{d\rho_i}{dt} + \Gamma_i\rho_i = Q_i + \sum_k A_{ki}\rho_k - 2\mathrm{Re}\left(i\sum_j V_{ij}\rho_{ji}\right), \quad (1)$$

$$\frac{d\rho_{ik}}{dt} + (\Gamma_{ik} + i\omega_{ik})\rho_{ik} = -i[V,\rho]_{ik}. \quad (2)$$

In equations (1), (2), the total derivative operator is $\frac{d}{dt} = \frac{\partial}{\partial t} + \upsilon\nabla$, Γ_i — level widths, Γ_{ik} — half-widths of transition lines, Q_i — excitation rates of levels in the absence of EM field, $V = -G\exp(i(\mathbf{k}\cdot\mathbf{r}) - \omega t)) + \mathrm{H.c.}$ — operator of atom-field interaction, $G = dE/2\hbar$, d — operator of generalized dipole moment, E — field strength vector, ω — frequency, $\mathbf{k}$ — wave vector of the wave, υ — atomic velocity vector. The term $\sum_k A_{ki}\rho_k$ in equations (1) determines the spontaneous decay of magnetic sublevels of the upper state m to the sublevels of the lower state n (the rate of this process is A_{mn}). We will solve the problem for stationary atoms. When solving the problem, an important value is $a_0 = A_{mn}/\Gamma_m$, called the radiation branching parameter from the upper state. On open transitions, the parameter $a_0 < 1$, and on closed transitions in the absence of collisions $a_0 = 1$. The

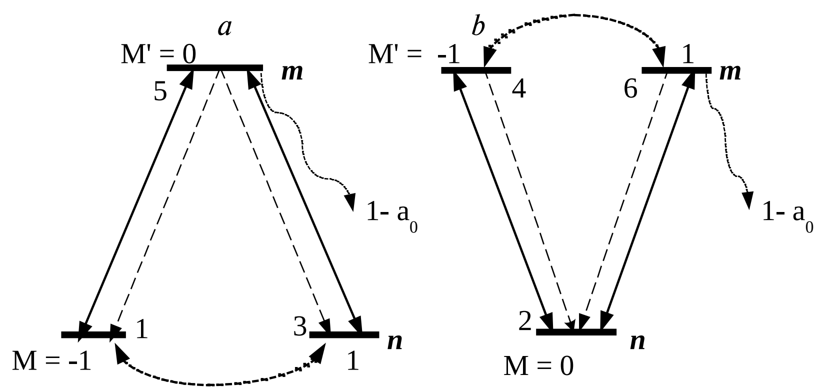

Fig. 1. Scheme of processes induced by linearly polarized EM field in Λ -types (*a*) and V-types (*b*) of atoms: solid lines stand for allowed transitions between magnetic sublevels in EM field; dotted lines stand for field-induced coherence of magnetic sublevels; dashed lines stand for spontaneous decay of sublevels of state*m* to sublevels of state *n* and other lower levels, $1 - a_0$ is the fraction of this process

value $1 - a_0$ determines the fraction of particles that decay from the upper m state to other lower-lying states. In closed transitions, the decay of the upper state occurs within the transition levels.

Solutions for non-diagonal elements of the density matrix in the field of a traveling EM wave can be represented $\rho_{ik} = R_{ik}\exp(-i(\omega t - \mathbf{k}\cdot\mathbf{r})) + \text{H.c.}$ [14, 20]. Then, in the stationary case from equations (1), (2) in Λ- and V-schemes (Fig. 1), we respectively obtain systems of algebraic equations

$$\begin{gathered}\Gamma_n\rho_k = Q_k + A_{5k}\rho_5 + 2\mathrm{Re}\left(iG_{k5}R_{5k}\right),\\ \Gamma_m\rho_5 = Q_5 + 2\mathrm{Re}\left(\sum_k iG_{5k}R_{k5}\right),\\ (\Gamma_{mn} - i\Omega_{5k})R_{5k} = -iG_{5k}(\rho_5 - \rho_k) + iG_{5l}r_{lk},\\ (\Gamma_n + i\omega_{kl})r_{kl} = i(G_{k5}R_{5l} - G_{5l}R_{k5}),\end{gathered} \tag{3}$$

$k = 1,3$, $l = 3,1$ in Λ-scheme and

$$\begin{gathered}\Gamma_n\rho_2 = Q_2 + \sum_k A_{k2}\rho_k + 2\mathrm{Re}\left(\sum_k iG_{2k}R_{k2}\right),\\ \Gamma_m\rho_k = Q_k + 2\mathrm{Re}(iG_{k2}R_{2k}),\\ (\Gamma_{mn} - i\Omega_{k2})R_{k2} = -iG_{k2}(\rho_k - \rho_2) - ir_{kl}G_{l2},\\ (\Gamma_m + i\omega_{kl})r_{kl} = i(G_{k2}R_{2l} - G_{2l}R_{k2}),\end{gathered} \tag{4}$$

$k = 4,6$, $l = 6,4$ in V-scheme. In equations (3), (4) ρ_i determine the populations of transition levels, R_{5k} and R_{k2} — are polarization coefficients of the atom at allowed transitions, $\Omega_{ik} = \omega - \omega_{ik}$ — are detunings of EM field frequency from frequencies ω_{ik} of transitions between sublevels of upper m and lower n states (in the absence of level splitting $\Omega_{ik} = \Omega_0 = \omega - \omega_{mn}$, where ω_{mn} are the frequences of unsplit transitions), r_{lk} are the polarization coefficients of atom at forbidden transitions, which determine EM field induced coherence (interference) of magnetic sublevels of lower or upper states, ω_{kl} are the frequencies of transitions between these sublevels.

After excluding from equation systems (3), (4) the terms caused by polarization coefficients R_{ik} and r_{lk}, we obtain systems of equations for level populations in the form

$$\begin{gathered}\Gamma_n\rho_k = Q_k + A_{5k}\rho_5 + (\rho_5 - \rho_k)\gamma_{5k} - (\rho_5 - \rho_l)\delta_{5l},\\ \Gamma_m\rho_5 = Q_5 - \sum_k[(\rho_5 - \rho_k)\gamma_{5k} - (\rho_5 - \rho_l)\delta_{5l}]\end{gathered} \tag{5}$$

in Λ-scheme, where

$$\begin{gathered}\gamma_{5k} = 2|G_{5k}|^2\ \mathrm{Re}\frac{1}{\alpha_{5k}},\\ \delta_{5l} = 2|G_{5k}|^2|G_{5l}|^2\ \mathrm{Re}\frac{1}{\alpha_{5k}(\Gamma_n + i\omega_{lk})\Gamma_{l5}},\\ \alpha_{5k} = \Gamma_{mn} - i\Omega_{5k} + \frac{|G_{5l}|^2}{\Gamma_n + i\omega_{lk}}\left(1 - \frac{|G_{5k}|^2}{(\Gamma_n + i\omega_{lk})\Gamma_{l5}}\right),\\ \Gamma_{5k} = \Gamma_{mn} - i\Omega_{5k} + \frac{|G_{5l}|^2}{\Gamma_n + i\omega_{lk}},\end{gathered} \tag{6}$$

and

$$\begin{gathered}\Gamma_n\rho_2 = Q_2 + \sum_k[A_{k2}\rho_k + (\rho_k - \rho_2)\gamma_{k2} - (\rho_l - \rho_2)\delta_{l2}],\\ \Gamma_m\rho_k = Q_k - [(\rho_k - \rho_2)\gamma_{k2} - (\rho_l - \rho_2)\delta_{l2}]\end{gathered} \tag{7}$$

in V-scheme, where

$$\begin{gathered}\gamma_{k2} = 2|G_{k2}|^2\ \mathrm{Re}\frac{1}{\alpha_{k2}},\\ \delta_{l2} = 2|G_{k2}|^2|G_{l2}|^2\ \mathrm{Re}\frac{1}{\alpha_{k2}(\Gamma_m + i\omega_{kl})\Gamma_{2l}},\\ \alpha_{k2} = \Gamma_{mn} - i\Omega_{k2} + \frac{|G_{l2}|^2}{\Gamma_m + i\omega_{kl}}\left(1 - \frac{|G_{k2}|^2}{(\Gamma_m + i\omega_{kl})\Gamma_{2l}}\right),\\ \Gamma_{k2} = \Gamma_{mn} - i\Omega_{k2} + \frac{|G_{l2}|^2}{\Gamma_m + i\omega_{kl}}.\end{gathered} \tag{8}$$

Values of indices in Λ- and V-schemes are indicated above.

Analytical solutions of equation systems (5), (7) in general form are complex for analysis. Therefore, their solutions use either numerical methods or approximations that allow analytical analysis in a limited range of values for atomic system parameters and EM-field intensity.

2.1 Analytical solutions of systems of equations (5), (7) considering the effect of MC levels

When solving equations (5), (7), as in the two-level system [13,14], we assume the level populations in the form: $\rho_i = N_i + r_i$, where N_i are level populations in the absence of EM field, and r_i are additions to populations due to this field's action. Then the values N_i and r_i will be determined by solutions of the following systems of equations:

$$\begin{gathered}\Gamma_n N_k = Q_k + A_{5k}N_5,\quad k = 1,3,\\ \Gamma_m N_5 = Q_5,\end{gathered} \tag{9}$$

$$(\Gamma_n + \gamma_{5i})r_i - \delta_{5k}r_k - (A_{5i} + \gamma_{5i} - \delta_{5k})r_5 = \\ = \gamma_{5i}\Delta N_{5i} - \delta_{5k}\Delta N_{5k}, i = 1,3, k = 3,1, \tag{10}$$

$$[\Gamma_m + \sum_{i=1,3}(\gamma_{5i} - \delta_{5i})]r_5 - \sum_{i=1,3}(\gamma_{5i} - \delta_{5i})r_i = \\ = -\sum_{i=1,3}(\gamma_{5i} - \delta_{5i})\Delta N_{5i}$$

in Λ-scheme and

$$\Gamma_n N_2 = Q_2 + \sum_{4,6} A_{k2}N_k, \\ \Gamma_m N_k = Q_k, \quad k = 4,6, \tag{11}$$

$$[\Gamma_n + \sum_{k=4,6}(\gamma_{k2} - \delta_{k2})]r_2 - \sum_{k=4,6}(A_{k2} + \gamma_{k2} - \delta_{k2})r_k = \\ = \sum_{k=4,6}(\gamma_{k2} - \delta_{k2})\Delta N_{k2}, \tag{12}$$

$$(\Gamma_m + \gamma_{i2})r_i - \delta_{k2}r_k - (\gamma_{i2} - \delta_{k2})r_2 = \\ = -(\gamma_{i2}\Delta N_{i2} - \delta_{k2}\Delta N_{k2}), i = 4,6, k = 6,4$$

in V-scheme. Here $\Delta N_{ik} = N_i - N_k$ are population differences between upper and lower levels in the absence of EM field. Further, we assume these population differences are equal: $\Delta N_{ik} = \Delta N$. Analytical solutions of systems (10), (12) in general form are expressed through ratios of third-degree polynomials, they are given in Appendix A. Solutions of these systems simplify in the absence of level splitting and with equal decay probabilities of levels and interaction parameters for each channel: at $\Omega_{51} = \Omega_{53} = \Omega_0$, $|G_{51}|^2 = |G_{53}|^2 = |G_\Lambda|^2$, $A_{51} = A_{53} = A_{5k}$ in Λ-scheme and $\Omega_{42} = \Omega_{62} = \Omega_0$, $A_{42} = A_{62} = A_{k2}$, $|G_{42}|^2 = |G_{62}|^2 = |G_V|^2$ in V-scheme. In this case, expressions for additions to level populations and their differences from Appendix A will be as follows:

$$r_5^0 = -\Delta N \frac{2\Gamma_n(\gamma_\Lambda - \delta_\Lambda)}{D_\Lambda^0}, \\ r_k^0 = \Delta N \frac{(\Gamma_m - 2A_{5k})(\gamma_\Lambda - \delta_\Lambda)}{D_\Lambda^0}, \\ D_\Lambda^0 = \Gamma_n\Gamma_m\left[1 + \frac{(\Gamma_m - 2A_{5k} + 2\Gamma_n)(\gamma_\Lambda - \delta_\Lambda)}{\Gamma_n\Gamma_m}\right], \\ \rho_5^0 - \rho_k^0 = \Delta N\left[1 - \frac{(\Gamma_m - 2A_{5k} + 2\Gamma_n)(\gamma_\Lambda - \delta_\Lambda)}{D_\Lambda^0}\right], \\ k = 1,3 \tag{13}$$

in Λ-scheme and

$$r_2^0 = \Delta N \frac{2(\Gamma_m - A_{k2})(\gamma_V - \delta_V)}{D_V^0}, \\ r_k^0 = -\Delta N \frac{\Gamma_n(\gamma_V - \delta_V)}{D_V^0}, \\ D_V^0 = \Gamma_n\Gamma_m\left[1 + \frac{(2\Gamma_m - 2A_{k2} + \Gamma_n)(\gamma_V - \delta_V)}{\Gamma_n\Gamma_m}\right], \\ \rho_k^0 - \rho_2^0 = \Delta N\left[1 - \frac{(2\Gamma_m - 2A_{k2} + \Gamma_n)(\gamma_V - \delta_V)}{D_V^0}\right], \\ k = 4,6 \tag{14}$$

in V-scheme. Here values γ_Λ, δ_Λ and γ_V, δ_V are determined by expressions (7), (8), in which splitting values for lower and upper levels should be taken as zero.

From expressions (13), (14) it follows that with radiative decay of levels on closed transitions (at $\Gamma_m = 2A_{5k} = A_{mn}$ in Λ-scheme or $\Gamma_m = A_{k2} = A_{mn}$ in V-scheme) additions to lower level populations, as in closed two-level system [13, 17], equal zero, and population changes under EM field action occur only at upper transition levels.

2.2 Analytical solutions of systems of equations (5), (7) without considering MC levels effect

In approximation without considering MC levels contribution to their population (such approximation is used in studying nonlinear resonance spectra on degenerate atomic transitions [3, 14, 20]) coefficient values in equations (10), (12) from (6), (8) are following:

$$\alpha_{5k}^0 = \Gamma_{mn} - i\Omega_{5k}, \\ \gamma_{5k}^0 = 2|G_{5k}|^2 \operatorname{Re}\frac{1}{\alpha_{5k}^0} = \frac{2|G_{5k}|^2\Gamma_{mn}}{\Gamma_{mn}^2 + \Omega_{5k}^2}, \\ \delta_{5l}^0 = 0, \quad k,l = 1,3$$

in Λ-scheme and

$$\alpha_{k2}^0 = \Gamma_{mn} - i\Omega_{k2}, \\ \gamma_{k2}^0 = 2|G_{k2}|^2 \operatorname{Re}\frac{1}{\alpha_{k2}^0} = \frac{2|G_{k2}|^2\Gamma_{mn}}{\Gamma_{mn}^2 + \Omega_{k2}^2}, \\ \delta_{k2}^0 = 0, \quad k = 4,6$$

in V-scheme. Then in this approximation systems of equations (10), (12) take form

$$
\begin{gathered}
(\Gamma_n + \gamma_{5k}^0) r_k - (A_{5k} + \gamma_{5k}^0) r_5 = \gamma_{5k}^0 \Delta N_{5k},\\
(\Gamma_m + \sum_k \gamma_{5k}^0) r_5 - \sum_k \gamma_{5k}^0 r_k = -\sum_k \gamma_{5k}^0 \Delta N_{5k},\\
k = 1,3
\end{gathered}
\quad (15)
$$

in Λ-scheme and

$$
\begin{gathered}
(\Gamma_n + \sum_k \gamma_{k2}^0 \gamma_{k2}^0) r_2 - \sum_k (A_{k2} + \gamma_{k2}^0) r_k =\\
= \sum_k \gamma_{k2}^0 \Delta N_{k2},\\
(\Gamma_m + \gamma_{k2}^0) r_k - \gamma_{k2}^0 r_2 = -\gamma_{k2}^0 \Delta N_{k2},\\
k = 4,6
\end{gathered}
\quad (16)
$$

in V-scheme.

Analytical solutions of systems (15), (16) are expressed through ratios of third-degree polynomials, they are given in Appendix B. The solutions of equations (15), (16) are also simplified in the absence of level splitting and when the probabilities of spontaneous decay of levels and interaction parameters for each channel are equal. In this case, the expressions for additions and differences in level populations from Appendix B will have the form

$$
\begin{gathered}
r_k^0 = \frac{\Delta N(\Gamma_m - 2A_{5k})}{\Gamma_m} \frac{\kappa_\Lambda \Gamma_{mn}^2}{\Gamma_{s1}^2 + \Omega_0^2},\\
r_5^0 = -\frac{\Delta N \Gamma_n}{\Gamma_m} \frac{2\kappa_\Lambda \Gamma_{mn}^2}{\Gamma_{s1}^2 + \Omega_0^2},\\
\rho_5^0 - \rho_k^0 = \Delta N \left[1 - \frac{\Gamma_m - 2A_{5k} + 2\Gamma_n}{\Gamma_m} \frac{\kappa_\Lambda \Gamma_{mn}^2}{\Gamma_{s1}^2 + \Omega_0^2}\right],\\
k = 1,3,
\end{gathered}
\quad (17)
$$

where

$$\Gamma_s^2 = \Gamma_{mn}^2 (1 + \kappa_\Lambda),$$

$$\Gamma_{s1}^2 = \Gamma_{mn}^2 \left[1 + \kappa_\Lambda \left(1 + 2\frac{\Gamma_n - A_{5k}}{\Gamma_m}\right)\right],$$

$$\kappa_\Lambda = 2 |G_{5k}|^2 / (\Gamma_{mn} \Gamma_n),$$

in Λ-scheme and

$$
\begin{gathered}
r_2^0 = \Delta N \frac{\beta\beta\kappa_V \Gamma_{mn}^2}{\Gamma_{s1}^2 + \Omega_0^2},\\
r_k^0 = -\Delta N \kappa_V \frac{\Gamma_{mn}^2}{\Gamma_s^2 + \Omega_0^2}\left[1 - \frac{\beta \Gamma_{mn}^2}{\Gamma_{s1}^2 + \Omega_0^2}\right],\\
\rho_k^0 - \rho_2^0 = \Delta N \left\{1 - \frac{\kappa_V (1+\beta) \Gamma_{mn}^2}{\Gamma_s^2 + \Omega_0^2}\left[1 - \frac{\kappa_V \beta \Gamma_{mn}^2}{\Gamma_{s1}^2 + \Omega_0^2}\right]\right\},\\
k = 4,6,
\end{gathered}
\quad (18)
$$

where

$$\Gamma_s^2 = \Gamma_{mn}^2 (1 + \kappa_V),$$

$$\Gamma_{s1}^2 = \Gamma_{mn}^2 [1 + \kappa_V (1 + \beta)],$$

$$\beta = 2(\Gamma_m - A_{k2}) / \Gamma_n,$$

$$\kappa_V = \frac{2 |G_{k2}|^2}{\Gamma_m \Gamma_{mn}},$$

in V-scheme. Hence, in the absence of collisions at closed transitions in Λ-scheme we have

$$
\begin{gathered}
\Gamma_m = 2A_{5k}, \quad r_k^0 = 0,\\
r_5^0 = -\frac{\Delta N \Gamma_n}{\Gamma_m} \frac{2\kappa_\Lambda \Gamma_{mn}^2}{\Gamma_{mn}^2 (1 + 2\kappa_\Lambda \Gamma_n / \Gamma_m) + \Omega_0^2},\\
\rho_5^0 - \rho_k^0 = \Delta N \left[1 - \frac{2\Gamma_n}{\Gamma_m} \frac{\kappa_\Lambda \Gamma_{mn}^2}{\Gamma_{mn}^2 (1 + 2\kappa_\Lambda \Gamma_n / \Gamma_m) + \Omega_0^2}\right],\\
k = 1,3;
\end{gathered}
$$

and in the case of V-scheme

$$
\begin{gathered}
\Gamma_m = A_{k2}, \quad \beta = 0, \quad r_2^0 = 0,\\
r_k^0 = -\Delta N \kappa_V \frac{\Gamma_{mn}^2}{\Gamma_{mn}^2 (1 + \kappa_V) + \Omega_0^2},\\
\rho_k^0 - \rho_2^0 = \Delta N \left[1 - \frac{\kappa_V \Gamma_{mn}^2}{\Gamma_{mn}^2 (1 + \kappa_V) + \Omega_0^2}\right],\\
k = 4,6.
\end{gathered}
$$

Thus in this approximation, as in the exact solution, the action of the EM field in closed Λ- and V-transitions in the absence of collisions does not change the populations of lower levels, as in works [13, 17, 21], and additions to the populations of upper levels and differences in their populations grow with increasing saturation parameters $\kappa_{\Lambda,V}$ (field intensity) according to a linear law at small values of parameters $\kappa_{\Lambda,V} \ll 1$ and reach a saturated value at large values $\kappa_{\Lambda,V} \gg 1$.

2.3 Results of numerical calculations of the contribution of the MC effect to level populations in Λ- and V-type transitions

Studies of the contributions of the MC effect of levels induced by the EM wave field of linear polarization to the saturation effect of level populations in (Λ)- and V-type transitions were conducted based on numerical solutions of equations systems (10)–(14) and their approximate analytical solutions (17), (18) with variation of EM field saturation parameters in the range of values $\kappa_V = 0.01–5$, ratios of level relaxation constants $\Gamma_n / \Gamma_m = 0.01–0.1$ and the magnitude of level splitting by magnetic field $\Delta_H / \Gamma_n = 0–50$ at closed and open ($a_0 = 0.8–0.9$) types of transitions. Several results of these calculations are presented in Figs. 2–5 at the ratio of relaxation constants $\Gamma_n / \Gamma_m = 0.1$. The figures show with dashed lines the results of numerical solutions to equations (10)–(14) taking into account the contribution of the MC levels effect, and with solid lines – solutions to equations (17), (18) without the contribution of this effect.

Analysis of both analytical and numerical calculations showed qualitative similarity in the manifestation of the level population saturation effect, including the manifestation of the MC

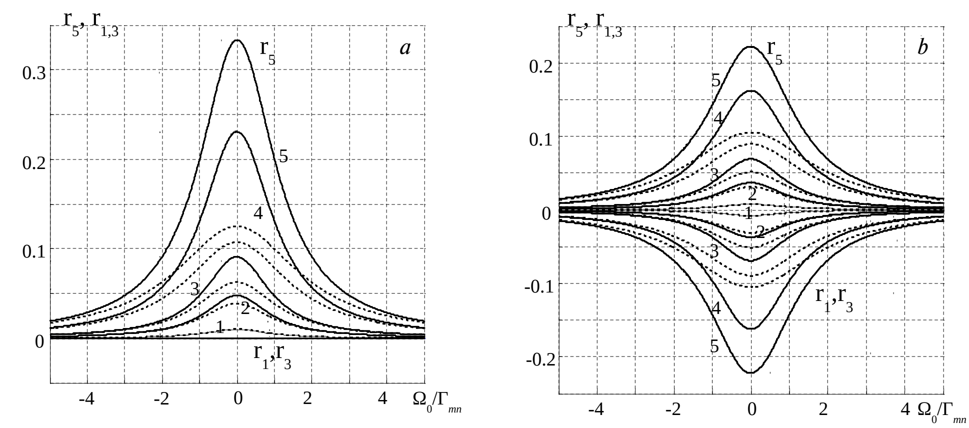

Fig. 2. Forms of additions to level populations in Λ-scheme at closed (*a*) and open (*b*, $a_0 = 0.8$) transitions: $\Gamma_n / \Gamma_m = 0.1$, $\kappa_\Lambda = 0.01$ (*1*), 0.05 (*2*), 0.1 (*3*), 0.3 (*4*), 0.9 (*5*). Dashed lines stand for the complete solution, solid lines stand for the solution without MC levels contribution

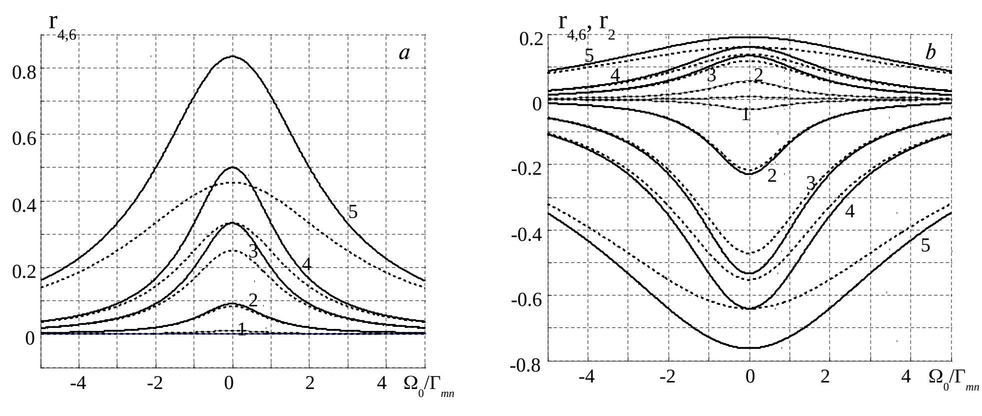

Fig. 3. Forms of additions to level populations in V-scheme at closed (*a*) and open (*b*, $a_0 = 0.8$) transitions: $\Gamma_n / \Gamma_m = 0.1$ $\kappa_V = 0.01$ (*1*), 0.1 (*2*), 0.9 (*3*), 1 (*4*), 5 (*5*). Dashed lines stand for the complete solution, solid lines stand for the solution without MC levels contribution

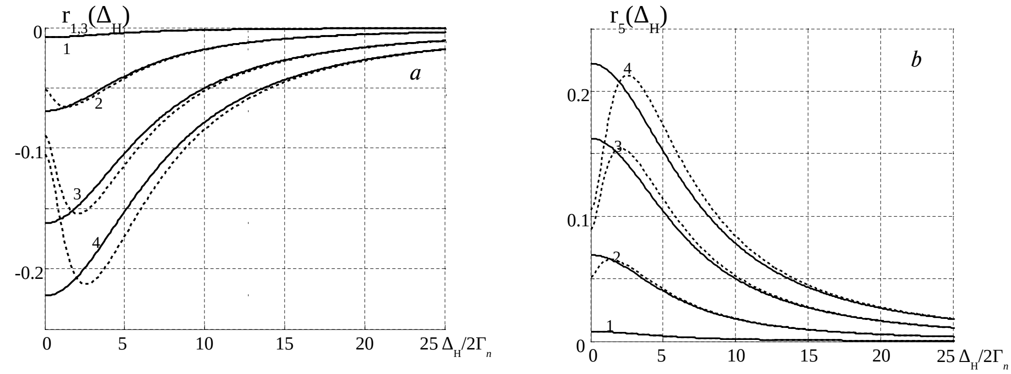

Fig. 4. Dependencies of additions to populations of lower (a) and upper (b) levels in Λ-scheme on the magnitude of level splitting Δ_H at $\Omega_0 = 0$, $a_0 = 0.8$, $\Gamma_n / \Gamma_m = 0.1$, $\kappa_\Lambda = 0.01$ (*1*), 0.1 (*2*), 0.3 (*3*), 0.9 (*4*). Dashed lines stand for the complete solution, solid lines stand for the solution without MC levels contribution

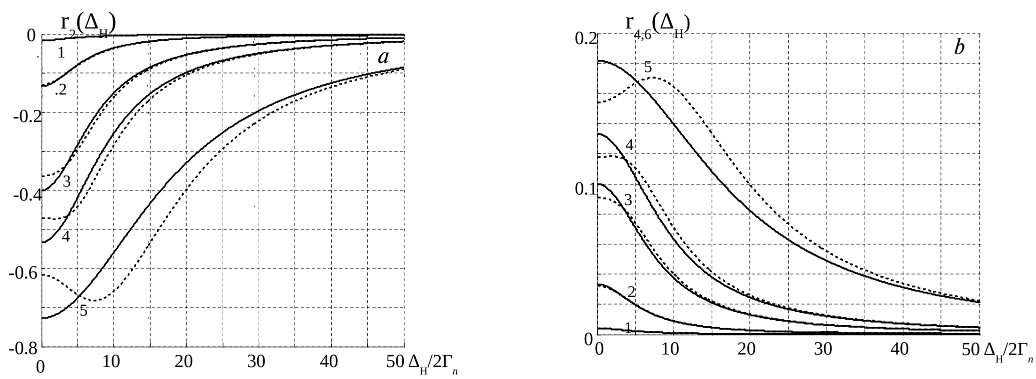

Fig. 5. Dependencies of additions to populations of lower (a) and upper (b) levels in V-scheme on the magnitude of level splitting Δ_H at $\Omega_0 = 0$, $a_0 = 0.8$, $\Gamma_n / \Gamma_m = 0.1$, $\kappa_V = 0.01$ (*1*), 0.1 (*2*), 0.9 (*3*), 1.0 (*4*), 5 (*5*). Dashed lines stand for the complete solution, solid lines stand for the solution without MC levels contribution

levels effect, under the action of EM field on the considered transitions, and the discovered differences are only quantitative in nature. First of all, we note the same character of changes (additions) in level populations depending on the degree of openness (parameter value a_0) of the atomic transition. On closed transitions in Λ- and V-schemes in the absence of level splitting, the EM field action does not affect the populations of lower levels (Figs. 2 *a*, 4 *a*), while the populations of upper levels increase with increasing intensity of $\kappa_{\Lambda,V}$ EM field parameters (curves 1–5). The dependencies show that the contribution of MC levels reduces the population of upper levels (dashed lines lie below solid ones). Moreover, in the Λ-scheme, the MC effect manifests in the population of the upper level at saturation parameter values $\kappa_\Lambda \geq 0.01$, and in the V-scheme – at values $\kappa_V \geq 0.1$. The magnitudes of MC contributions grow with increasing saturation parameter values, and their share in the field-formed level population can be determining. Thus, in the Λ-scheme at parameter values $\kappa_\Lambda = 0.3$–0.9 (Fig. 2 *a*, curves *4*, *5*) the additions to the upper level population at the line center due to the MC effect constitute more than 50% of the field-saturated level population without accounting for the MC effect. In the case of V-scheme (Fig. 3 *a*, curves *4*, *5*) the maximum contribution of the addition is realized at parameters $\kappa_V = 1$–5 and reaches $\sim (30$–$50)\%$ of the level population values without the MC effect contribution. Meanwhile, the MC effect contribution reduces the absolute values of upper level populations.

As noted above, the absence of EM field influence on lower level populations in closed Λ- and V-type transitions was also found in works [13, 17, 21] and is a general property of closed transitions.

In the case of open Λ- and V-type transitions, the EM field action affects the populations of all transition levels: with increasing field intensity (parameters $\kappa_{\Lambda,V}$) upper level populations increase while lower level populations decrease (Figs. 2 *b*, 3 *b*). Moreover, according to the provided data, MC level contributions reduce the magnitude of additions in populations of both lower and upper levels, thereby increasing the populations of lower levels and decreasing these values at upper levels of both transition types Furthermore, in open transitions, the MC effect manifests in level populations at higher intensities (values of parameters $\kappa_{\Lambda,V}$ of EM field) than in closed transitions. At the same parameter values $\kappa_{\Lambda,V}$ the magnitudes of MC contributions to level populations are smaller than in closed transitions. Thus, in transitions with branching parameter $a_0 = 0.8$ in Λ-scheme, the MC effect appears in level populations at values $\kappa_\Lambda \geq 0.05$, and in V-scheme – at $\kappa_V > 0.1$. Meanwhile, in Λ-scheme, the maximum MC contribution to populations of all levels is $\sim 50\%$ (Fig. 2 *b*, curves *4*, *5*, $\kappa_\Lambda = 0.3–0.9$),and in V-scheme (Fig. 3*b*, curves *5*, $\kappa_V = 5$) this value is $\leq 18\%$ (for lower level) and less than 15% (for upper levels) of the level population values without considering the MC effect. Note that the MC contribution decreases the differences in transition level populations and thereby increases the EM wave absorption coefficient.

The influence of level splitting (by magnetic field) on the magnitude of additions in level populations in Λ- and V-schemes under linearly polarized EM field action is shown in Fig. 4 and 5 for the line center (at $\Omega_0 = 0$) of open transition ($a_0 = 0.8$) at different values of parameters $\kappa_{\Lambda,V}$ of EM field. In closed transitions, the behavior of additions in upper level populations depending on the magnitude of level splitting practically coincides with the behavior of additions for upper levels of open transitions with $a_0 = 0.8$.

From Figs. 4 and 5, it follows that the dependencies of population additions to energy levels, including those due to the MC effect, on the magnitude of level splitting in Λ- and V-schemes have a similar form, with only quantitative differences in the magnitude of additions, ranges of level splitting, and intensities (saturation parameters) of the EM field at which the MC effect manifests. Thus, in the Λ-scheme, the influence of MC on the populations of split levels is detected at parameter values $\kappa_\Lambda > 0.01$ (Fig. 4, curves *2–4*), and in the V-scheme – at values $\kappa_V \geq 0.9$ (Fig. 5, curves *2–4*). At small level splittings $\Delta_H < (2–5)\Gamma_n$ in the Λ-scheme and $\Delta_H < (7–10)\Gamma_n$ in the V-scheme, the contribution of the MC effect leads to a decrease in population additions at all levels of the considered transitions. At level splittings $\Delta_H > (2–5)\Gamma_n$ in the Λ-scheme and $\Delta_H > (7–10)\Gamma_n$ in the V-scheme, the MC effect additions change sign, leading to a small increase in upper level populations (dashed lines above solid ones) and a decrease in lower level populations (here dashed lines are below). The critical splitting values at which the additions change sign depend on the saturation parameter values and change (increase) in the specified ranges with increasing parameter values κ_Λ and κ_V.

In the case of the Λ-scheme, the magnitude of the MC contribution is maximal at small level splittings $\Delta_H \sim 0$ (Fig. 4, curves 4) and amounts to more than 50% (as well as in Fig. 2b) relative to the level population without accounting for the effect contribution, while at level splittings $\Delta_H \sim (7–10)\Gamma_n$ the maximum MC contribution is less and amounts to $\sim 20\%$ of the above value.

In the case of the V-scheme (Fig. 5), at small level splittings, the MC additions to level populations are significantly smaller than in the Λ-scheme, and at parameter $\kappa_V = 5$ (curves 5) amount to $\leq 18\%$ for the lower level and less than 15% for the upper levels, while at large splittings $\Delta_H \approx (2–3)\Gamma_m$ the maximum MC contributions reach values of $\sim (15–20)\%$ relative to the additions without accounting for the MC effect. It should be emphasized that for all types of transitions, MC contributions in the region of small level splittings lead to a decrease in upper level populations and an increase in lower level populations, while in the region of large splittings – to an increase in upper level populations and a decrease in lower level populations.

3. MC LEVELS EFFECT IN ABSORPTION SPECTRA OF LINEARLY POLARIZED EM WAVES IN Λ- AND V-TYPE TRANSITIONS DURING FREQUENCY AND MAGNETIC SCANNING

3.1 Absorption line shapes of linearly polarized EM waves in Λ- and V-type transitions during frequency and magnetic scanning

The absorption line shapes of linearly polarized EM waves during frequency or magnetic scanning are determined through the EM field work by the following expression [14]:

$$\frac{\alpha_s(\Omega)}{\alpha_0} = -\Gamma_{mn}\langle \mathrm{Re}(i\sum_{i,k} R_{ik}G_{ki}/|G|^2)\rangle, \quad (19)$$

where $\alpha_0 = 4\pi\omega_{mn}d^2/c\hbar\Gamma_{mn}$ — is the resonant absorption cross-section, and values R_{ik} are determined by solutions of equations systems (3)–(7) in corresponding approximations. With exact solution of these equations (considering MC contribution to level populations), analytical expressions for absorption line shapes (19), like expressions for level populations (Appendix A), are complex and difficult to analyze. In this case, line shapes were determined based on expression (19) and numerical solutions of equations systems (3)–(7) with variation of atomic transition parameters and EM field intensity (saturation parameters).

In approximation without considering MC contribution to level populations, analytical expressions for absorption line shapes in Λ- and V-type transitions can be represented as

$$\frac{\alpha^1_{s\Lambda}(\Omega)}{\alpha_0} = -\Gamma_m \mathrm{Re}\sum_{k,l}\left(\frac{1}{\Gamma_{mn} - i\Omega_{5k} + \dfrac{|G_{5l}|^2}{\Gamma_n + i\omega_{lk}}}\left[(\rho^0_5 - \rho^0_k) - \frac{(\rho^0_5 - \rho^0_l)|G_{5l}|^2}{(\Gamma_n + i\omega lk)(\Gamma_{mn} + i\Omega_{5l})}\right]\right), \quad (20)$$

$$\frac{\alpha^1_{sV}(\Omega)}{\alpha_0} = -\Gamma_m \mathrm{Re}\sum_{k,l}\left(\frac{1}{\Gamma_{mn} - i\Omega_{k2} + \dfrac{|G_{l2}|^2}{\Gamma_m + i\omega_{kl}}}\left[(\rho^0_k - \rho^0_2) - \frac{(\rho^0_l - \rho^0_2)|G_{l2}|^2}{(\Gamma_m + i\omega_{kl})(\Gamma_{mn} + i\Omega_{l2})}\right]\right), \quad (21)$$

where level population differences are determined by expressions (B.1), (B.2) of Appendix B. Expressions (20), (21), like expressions for population differences, take simple form when interaction parameters and spontaneous decay probabilities are equal for each transition channel: at $|G_{51}|^2 = |G_{53}|^2 = |G_\Lambda|^2$, $A_{51} = A_{53}$ (in Λ-scheme) and $|G_{42}|^2 = |G_{62}|^2 = |G_V|^2$, $A_{42} = A_{62}$ (in V-scheme). Further we will consider transitions with such parameters.

During frequency scanning in absence of level splitting ($\omega_{kl} = 0$) frequency detunings $\Omega_{ik} = \Omega_0$, and absorption line shapes from (20), (21) will be as follows:

$$\frac{\alpha^1_{s\Lambda}(\Omega_0)}{\alpha_0} = -2\Gamma_m\Delta N\left[1 - \frac{\Gamma_m - 2A_{51} + 2\Gamma_n}{\Gamma_m}\frac{\kappa_\Lambda\Gamma^2_{mn}}{\Gamma^2_{s1} + \Omega^2_0}\right] \times \mathrm{Re}\left\{\frac{1}{\Gamma_{mn}(1 + 0.5\kappa_\Lambda) - i\Omega_0}\left[1 - \frac{0.5\kappa_\Lambda\Gamma_{mn}}{\Gamma_{mn} + i\Omega_0}\right]\right\}, \quad (22)$$

where

$$\Gamma^2_{s1} = \Gamma^2_{mn}\left[1 + \kappa_\Lambda\left(1 + 2\frac{\Gamma_n - A_{51}}{\Gamma_m}\right)\right],$$

$$\kappa_\Lambda = \frac{2|G_{5k}|^2}{\Gamma_n\Gamma_{mn}},$$

in Λ-scheme and

$$\frac{\alpha^1_{sV}(\Omega_0)}{\alpha_0} = -2\Gamma_m\Delta N[1 - \frac{\kappa_V(1+\beta)\Gamma^2_{mn}}{\Gamma^2_s + \Omega^2_0}\left(1 - \frac{\kappa_V\beta\Gamma_{mn}{}^2}{\Gamma^2_{s1} + \Omega^2_0}\right)] \times \mathrm{Re}\{\frac{1}{\Gamma_{mn}(1 + 0.5\kappa_V) - i\Omega_0}\left[1 - \frac{0.5\kappa_V\Gamma_{mn}}{\Gamma_{mn} + i\Omega_0}\right]\}, \quad (23)$$

where

$$\Gamma^2_s = \Gamma^2_{mn}(1 + \kappa_V),$$

$$\Gamma^2_{s1} = \Gamma^2_{mn}[1 + \kappa_V(1 + \beta)],$$

$$\beta = 2\frac{\Gamma_m - A_{k2}}{\Gamma_n}, \quad \kappa_V = \frac{2|G_{k2}|^2}{\Gamma_m\Gamma_{mn}},$$

in V-scheme.

Hence on closed transitions absorption line shapes can be represented as

$$\frac{\alpha^1_{s\Lambda}(\Omega_0)}{\alpha_0} \approx -2\Gamma_m\Delta N\frac{\Gamma_{mn}(1 + 0.5\kappa_\Lambda)}{\Gamma^2_{mn}(1 + 0.5\kappa_\Lambda)^2 + \Omega^2_0} \times \left[1 - \frac{0.5\kappa_\Lambda\Gamma^2_{mn}}{\Gamma^2_{mn} + \Omega^2_0}\right] \times \left[1 - \frac{2\Gamma_n}{\Gamma_m}\frac{\kappa_\Lambda\Gamma^2_{mn}}{\Gamma^2_{mn}(1 + 2\kappa_\Lambda\Gamma_n/\Gamma_m) + \Omega^2_0}\right] \quad (24)$$

in Λ-scheme and

$$\frac{\alpha^1_{sV}(\Omega_0)}{\alpha_0} \approx -2\Gamma_m \Delta N \frac{\Gamma_{mn}(1+0.5\kappa_V)}{\Gamma^2_{mn}(1+0.5\kappa_V)^2+\Omega_0^2}\times \left[1-\frac{0.5\kappa_V\Gamma^2_{mn}}{\Gamma^2_{mn}+\Omega_0^2}\right]\left[1-\frac{\kappa_V\Gamma^2_{mn}}{\Gamma^2_{mn}(1+\kappa_V)+\Omega_0^2}\right] \tag{25}$$

in V-scheme.

During magnetic scanning at the center of unsplit transition line (at $\Omega_0 = 0$) frequency detunings Ω_{ik} in expressions (20), (21) are determined by splitting ω_{kl} of lower or upper levels as $\Omega_{ik} = \pm\Delta_H/2$ ($\Delta_H = |\omega_{kl}|$). In this case absorption line shapes can be represented as

$$\frac{\alpha^1_{s\Lambda}(\Delta_H)}{\alpha_0} = -\Delta N \frac{2\Gamma_m\Gamma_{mn}}{\Gamma^2_{mn}+\Delta_H^2/4}\times \left[1-\frac{\kappa_\Lambda\Gamma_n^2\Gamma^2_{mn}}{(\Gamma_n^2+\Delta_H^2)(\Gamma^2_{mn}+\Delta_H^2/4)}\right]\times \left[1-\frac{\Gamma_m-2A_{51}+2\Gamma_n}{\Gamma_m}\frac{\kappa_\Lambda\Gamma^2_{mn}}{\Gamma^2_{s1}+\Delta_H^2/4}\right], \tag{26}$$

where

$$\Gamma^2_{s1} = \Gamma^2_{mn}\left[1+\kappa_\Lambda\left(1+2\frac{\Gamma_n-A_{51}}{\Gamma_m}\right)\right],$$

in Λ-scheme and

$$\frac{\alpha^1_{sV}(\Delta_H)}{\alpha_0} = -\Delta N \frac{2\Gamma_m\Gamma_{mn}}{\Gamma^2_{mn}+\Delta_H^2/4}\times \left[1-\frac{\kappa_V\Gamma_m^2\Gamma^2_{mn}}{(\Gamma_m^2+\Delta_H^2)(\Gamma^2_{mn}+\Delta_H^2/4)}\right]\times \left[1-\frac{(1+\beta)\kappa_V\Gamma^2_{mn}}{\Gamma_s^2+\Delta_H^2/4}\left(1-\frac{\beta\kappa_V\Gamma^2_{mn}}{\Gamma^2_{s1}+\Delta_H^2/4}\right)\right], \tag{27}$$

where

$$\Gamma_s^2 = \Gamma^2_{mn}(1+\kappa_V),$$

$$\Gamma^2_{s1} = \Gamma^2_{mn}[1+\kappa_V(1+\beta)],$$

$$\beta = 2\frac{\Gamma_m - A_{k2}}{\Gamma_n},$$

in V-scheme.

From here, the closed transitions of the absorption line shapes during magnetic scanning in Λ- and V-schemes are determined respectively as

$$\frac{\alpha^1_{s\Lambda 0}(\Delta_H)}{\alpha_0} = -\Delta N \frac{2\Gamma_m\Gamma_{mn}}{\Gamma^2_{s\Lambda}+\Delta_H^2/4}\times \left[1-\frac{\kappa_\Lambda\Gamma_n^2\Gamma^2_{mn}}{(\Gamma_n^2+\Delta_H^2)(\Gamma^2_{mn}+\Delta_H^2/4)}\right], \quad \Gamma^2_{s\Lambda} = \Gamma^2_{mn}\left(1+2\kappa_\Lambda\frac{\Gamma_n}{\Gamma_m}\right), \tag{28}$$

$$\frac{\alpha^1_{sV0}(\Delta_H)}{\alpha_0} = -\Delta N \frac{2\Gamma_m\Gamma_{mn}}{\Gamma^2_{sV}+\Delta_H^2/4}\times \left[1-\frac{\kappa_V\Gamma_m^2\Gamma^2_{mn}}{(\Gamma_m^2+\Delta_H^2)(\Gamma^2_{mn}+\Delta_H^2/4)}\right], \quad \Gamma^2_{sV} = \Gamma^2_{mn}(1+\kappa_V). \tag{29}$$

From expressions

it follows that the absorption line shapes during magnetic scanning in Λ- and V-type transitions in the approximation without considering the MC effect manifest as Lorentzian peaks, whose widths and amplitudes depend on the intensity (saturation parameters) of the EM field. With saturation parameters $\kappa_{\Lambda,V} \ll 1$ as their values increase, the peak widths grow according to the root law, while peak amplitudes decrease linearly. Near the peak centers, dips are formed: in the Λ-scheme – with a half-width of the lower level Γ_n, and in the V-scheme – with a half-width of the upper level Γ_m. Therefore, with the ratio $\Gamma_n \ll \Gamma_m$ the dip width in the Λ-scheme is significantly smaller, and its contrast is significantly greater, and it manifests at lower saturation parameters (intensities) of the EM field than in the V-scheme.

Note that the physical reason for the formation of dips with half-width of the lower or upper level in the magnetic scanning line shape is the polarization induced by the linearly polarized field on forbidden transitions between levels of the lower or upper state of the considered atom, and these dips are coherent in nature.

3.2 Results of numerical studies of the MC levels effect contribution to the absorption line shape of a linearly polarized wave during frequency and magnetic scanning on Λ- and V-type transitions

Studies of MC levels contributions, induced by linearly polarized EM field in Λ- and V-type

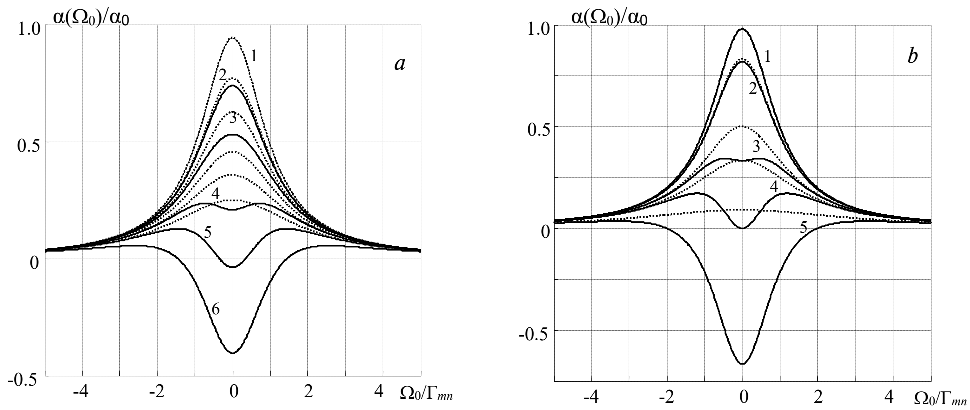

Fig. 6. Absorption line shapes during frequency scanning in Λ-scheme (*a*) and V-scheme (*b*) at a_0 = 1, Γ_n / Γ_m = 0.1. *a* — κ_Λ = 0.01 (*1*), 0.05 (*2*), 0.1 (*3*), 0.2 (*4*), 0.3 (*5*), 0.9 (*6*); *b* — κ_V = 0.01 (*1*), 0.1 (*2*), 0.9 (*3*), 1 (*4*), 5 (*5*). Dashed lines stand for the complete solution, solid lines stand for the without MC levels contribution

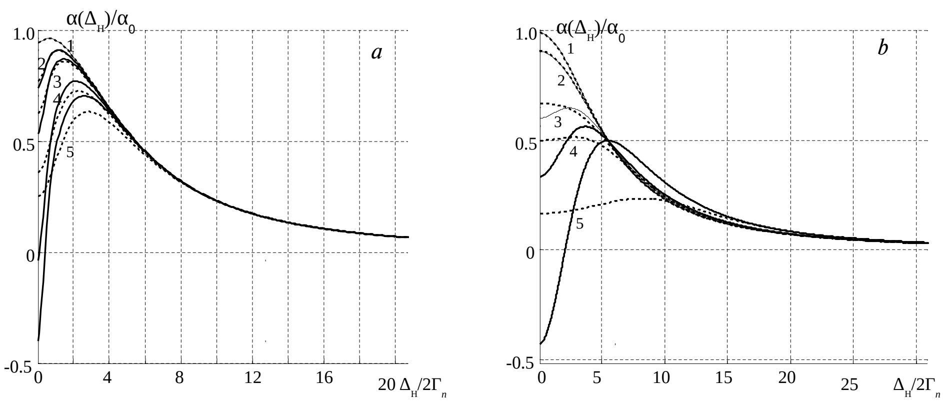

Fig. 7. Absorption line shapes during magnetic scanning in Λ-scheme (*a*) and V-scheme (*b*) at a_0 = 1, Γ_n / Γ_m = 0.1, Γ_{mn} = 5.5Γ_n. *a* — κ_Λ = 0.01(*1*), 0.05 (*2*), 0.1 (*3*), 0.3 (*4*), 0.9 (*5*); *b* — κ_V = 0.01 (*1*), 0.1 (*2*), 0.9 (*3*), 1 (*4*), 5 (*5*). Dashed lines – stand for the complete solution, solid lines – stand for the without MC levels contribution

transitions, to the absorption spectra of this wave during frequency and magnetic scanning were conducted, as mentioned above, based on expression (19) and numerical solutions of equations (3)–(7), or their approximate solutions (22)–(29) with variation of EM field saturation parameters in the range of values $\kappa_{\Lambda,V}$ = 0.01–5, relaxation constants ratio Γ_n / Γ_m = 0.1–0.01 and level splitting values Δ_H / Γ_n = 0–50 on closed and open (a_0 = 0.8–0.9) types of transitions. Analysis of research results showed that the nature of MC levels contributions to absorption line shapes both during frequency and magnetic scanning in Λ- and V-schemes is qualitatively similar for open and closed transitions, with only small quantitative differences. Therefore, the figures below show results for closed transitions with constants ratio Γ_n / Γ_m = 0.1. Dashed lines in the figures correspond to numerical solutions taking into account the MC levels effect, while solid lines represent solutions without this effect's contribution.

The absorption line shapes during frequency scanning are shown in Fig. 6. At low EM-field intensities (parameters $\kappa_{\Lambda,V}$ < 0.01) absorption lines appear near the atomic transition frequency as a Lorentzian peak with transition half-width Γ_{mn} (curves 1). With increasing EM-field intensity (at values $\kappa_{\Lambda,V}$ > 0.01) there is a decrease in absorption coefficients (curves 2, 3) due to the decrease in level population differences (population saturation effect) and an increase in spectral line width. Moreover, at saturation parameter values $\kappa_\Lambda \leq 0.05$ in Λ-scheme and $\kappa_V \leq 0.1$ in V-scheme, the line shapes are described by expressions (24) and (25) respectively, obtained without considering the MC levels effect. In this case, the absorption resonance amplitudes decrease according to the linear law $\sim \beta\kappa_{\Lambda,V}$, where $\beta \approx 1$ (in Λ-scheme) and $\beta \approx 2$ (in V-scheme), and the resonance widths follow the root ($\sim \sqrt{1+\kappa_{\Lambda,V}}$) dependence, as in a two-level system [14]. At saturation parameter values $\kappa_\Lambda > 0.05$ (in Λ-scheme) and $\kappa_V > 0.1$ (in V-scheme), differences in the behavior of absorption line shapes of different approximations are observed, which is due to the manifestation of MC levels. As shown in section 2, the contribution of MC levels leads to an increase in their population difference, which manifests in increased absorption at transitions (on graphs, dashed lines lie above solid ones), as well as in slight narrowing of absorption lines. The relative changes in absorption magnitude at line center due to MC levels, according to Fig. 6, can be $\sim (75–100)\%$ (curves 3, 4). In Λ-scheme, this is realized at saturation parameter values $\kappa_\Lambda \geq 0.3$, and in V-scheme – at values $\kappa_V \geq 1$.

Analysis of absorption line shapes taking into account the contribution of MC levels (Fig. 6, dashed lines) showed that with parameter values $\kappa_{\Lambda,V} > 0.05$ half-width resonances in Λ-scheme follow a linear law $\Gamma \approx \Gamma_{mn}(1+2\kappa_\Lambda)$, and in V-scheme – a square root law $\Gamma \approx \Gamma_{mn}\sqrt{1+\kappa_V}$. The resonance amplitudes decrease nonlinearly.

Note that in the approximation without considering the contribution of MC levels at the center of absorption lines with saturation parameters $\kappa_\Lambda > 0.1$ (in Λ-scheme) and (in V-scheme), dips are formed (Fig. 6, solid lines 3, 4), whose amplitudes with increasing parameters $\kappa_{\Lambda,V}$ take negative values (curves 5). This indicates the inapplicability of this approximation in the specified range of saturation parameters (intensities) of the EM field. In solutions considering MC contributions to level populations, no splitting in absorption line shapes or regions with negative absorption occurs (dashed lines 3-5).

Absorption line shapes during magnetic scanning are shown in Fig. 7. At low EM field intensities (saturation parameters $\kappa_\Lambda < 0.01$ in Λ-scheme and $\kappa_V \leq 0.1$ in V-scheme), absorption lines appear near zero magnetic field as a Lorentzian peak with transition half-width Γ_{mn} (curves *1*). With increasing intensity (parameters $\kappa_{\Lambda,V}$) peak amplitudes decrease, and at saturation parameters $\kappa_\Lambda > 0.01$ (in Λ-scheme) and $\kappa_V > 0.1$ (in V-scheme), dips form near zero magnetic field in the line shapes, whose amplitudes and widths depend on of level relaxation constants, atomic transition type, and EM field intensity. The common feature is that the contribution of the MC levels effect to magnetic scanning line shapes at any transitions (dashed curves 2-5) leads to decreased amplitudes and increased widths of absorption line structures (in the form of peaks and dips), while reducing the contrast of these structures.

In the case of Λ-transitions scheme (Fig. 7 *a*), a strong dependence of the dip parameters on the ratio of level relaxation constants is observed Thus, with the ratio of relaxation constants $\Gamma_n / \Gamma_m \ll 1$ we have a narrow dip against the background of a wide peak in the line shape, and with parameters $\kappa_\Lambda \leq 0.1$ (curves *1–3*) the resonance shape is well described by expression (28) without considering the contribution of the MC effect. When the lower levels split $\Gamma_{mn} \gg \Delta_H \sim \Gamma_n$ the shape of the narrow dip (near the line center) is determined as

$$\frac{\alpha^1_{s\Lambda 0}(\Delta_H)}{\alpha_0} = -\Delta N \frac{2\Gamma_m}{\Gamma_{mn}}\left[1 - \frac{\kappa_\Lambda \Gamma_n^2}{\Gamma_n^2 + \Delta_H^2}\right], \quad (30)$$

i.e., we have a dip with a half-width determined by the relaxation constant of the lower level Γ_n, whose amplitude increases while the contrast decreases linearly with increasing value κ_Λ. At level splittings $\Gamma_n \ll \Delta_H \sim \Gamma_{mn}$ the resonance shape will be determined by the wing of the peak Lorentzian (28) in the form

$$\frac{\alpha^1_{s\Lambda 0}(\Delta_H)}{\alpha_0} = -\Delta N \frac{2\Gamma_m\Gamma_{mn}}{\Gamma_{s\Lambda}^2 + \Delta_H^2 / 4} \times \left[1 - \frac{\kappa_\Lambda \Gamma_n^2 \Gamma_{mn}^2}{\Delta_H^2(\Gamma_{mn}^2 + \Delta_H^2 / 4)}\right]. \quad (31)$$

In this case, with increasing parameter κ_Λ the width of the peak part of the resonance grows according to the root law, while the amplitude decreases linearly. The maximum peak value depends on the parameter value κ_Λ and is found from relation (28) by solving a cubic equation. With saturation parameters $\kappa_\Lambda > 0.1$ the contribution of MC levels to the resonance shape becomes significant, which is manifested in the difference between the numerical solution (dashed curves 4, 5) and the analytical solution (28) (solid curves). A significant difference is observed in the amplitude of the narrow dip, its width values, and contrast. Thus, when changing the values κ_Λ in the range 0.1–0.3 the amplitude and contrast of the dip decrease approximately by 2 times, while its width increases by more than 2 times (curve 4). The changes in the resonance wing due to the contribution of MC levels are manifested as a slight decrease in the peak amplitude and a shift of its maximum towards larger values of level splittings.

In the case of a V-scheme transition (Fig. 7 *b*), a dip is also formed in the magnetic scanning line shape near its center at saturation parameters $\kappa_V > 0.1$ with its width being significantly larger and its amplitude and contrast significantly lower than those of a similar dip in the Λ-scheme. The influence of the MC levels effect on the dip shape is detected at parameter values $\kappa_V > 0.1$ (curves *3–5*). Moreover, at values $0.3 \le \kappa_V \le 1$ (curves *3*, *4*) the action of the MC levels effect leads to a decrease in the dip amplitude and especially its contrast in the line center, but weakly affects the line wing. At saturation parameters $\kappa_V > 1$ the contribution of MC levels becomes important in forming the spectrum of the entire resonance (curve *5*). In this case, the effect influences both the amplitude and width of the dip at splittings $\Delta_H < \Gamma_{mn}$, and the line wing structures at $\Delta_H > \Gamma_{mn}$. It should be noted that accounting for MC levels in absorption spectra during magnetic scanning, as well as during frequency scanning (see above), prevents the occurrence of anomalies in resonance shapes that arise in approximations that do not take into account the contribution of the MC levels effect (Figs. 5 *a*, *b*, curves *5*).

4. CONCLUSIONS

Thus, the presented results of numerical and analytical studies of MC levels induced by linearly polarized EM field in Λ- and V-type transitions demonstrate the important role of this effect in forming both the population of transition levels and EM field absorption spectra during frequency and magnetic scanning. Under optimal conditions, the contribution of the MC effect can constitute more than 50% of the populations of levels under conditions without considering the MC contribution and lead to (75–100)-percent changes in absorption coefficients at line centers during frequency and magnetic scanning The Λ-scheme is more critical in this case, where the manifestation of the MC effect in level populations and absorption spectra is detected at significantly lower saturation parameters (intensities) of the EM field and in a narrower range of level splittings. Thus, in the Λ-scheme, the splitting range near the line center was determined by the relaxation constant of the lower level and amounted to $\sim 2\Gamma_n$, while in the V-scheme, this range was determined by the constant of the upper level and amounted to $\sim \Gamma_m$. Using calculations that do not take into account the contribution of the MC levels effect induced by linearly polarized EM field to level populations in Λ-type transitions leads to significant errors in determining both the populations of these levels and the results of processes depending on level populations even at low saturation parameters (intensities) of the EM field In particular, this is detected in the shapes of EM field absorption lines during frequency and magnetic scanning. When the contribution of MC levels is taken into account in the solutions, no anomalies arise in the shapes of nonlinear absorption lines.

Attention should be paid to the dips with the width of the lower level Γ_n (in Λ-scheme) or with the width of the upper level Γ_m (in V-scheme) in the absorption line shapes during magnetic scanning near zero splitting of transition levels. As noted, the cause of these structures in absorption line shapes is coherence induced by a linearly polarized field on forbidden transitions between magnetic sublevels of lower or upper states in the considered three-level atoms, and these structures are coherent in nature. Resonances with lower level width appeared in saturated absorption spectra of the probe wave during magnetic scanning in atoms with more complex level structure [17–19, 21]. In these works, it was noted that these resonances were caused by the action of the saturating wave field and were also coherent in nature.

In conclusion, we note that the narrow resonance occurring in the absorption spectrum of a traveling linearly polarized EM wave in an atom with Λ-scheme of levels during magnetic scanning may be of interest for several practical applications, particularly for measuring weak magnetic fields.

FUNDING

The work was carried out within the State Assignment of IAE SB RAS (project No. 1210317000304) and IPS SB RAS (project No. FWGW-2021-0012).

APPENDIX A

In Λ-scheme, solutions of the equation system (11) are as follows:

$$r_k = \frac{\Delta N}{D_\Lambda}\{(\Gamma_m + \gamma_s)\times$$
$$\times[(\Gamma_n + \gamma_{5l})(\gamma_{5k} - \delta_{5l}) + (\gamma_{5l} - \delta_{5k})\delta_{5l}] -$$
$$-A^s_{5k}[(\Gamma_n + \gamma_{5l})\gamma_s - (\gamma_{5l} - \delta_{5l})\delta_{5l}] -$$
$$-A^s_{5l}[(\gamma_{5l} - \delta_{5l})(\gamma_{5k} - \delta_{5l}) + \delta_{5l}\gamma_s)]\},$$
$$k = 1,3, \quad l = 3,1, \tag{A.1}$$

$$r_5 = -\frac{\Delta N\Gamma_n}{D_\Lambda}[(\Gamma_n + \gamma_{51} + \delta_{53})(\gamma_{53} - \delta_{51}) +$$
$$+(\Gamma_n + \gamma_{53} + \delta_{51})(\gamma_{51} - \delta_{53})],$$

$$D_\Lambda = \Gamma_n(\Gamma_n + \gamma_{51} + \gamma_{53})(\Gamma_m + \gamma_s) +$$
$$+(\Gamma_m - A_{51} - A_{53})(\gamma_{51}\gamma_{53} - \delta_{51}\delta_{53}) -$$
$$-\Gamma_n[A^s_{51}(\gamma_{51} - \delta_{51}) + A^s_{53}(\gamma_{53} - \delta_{53})],$$

$$\gamma_s = \gamma_{51} + \gamma_{53} - \delta_{51} - \delta_{53},$$

$$A^s_{5k} = A_{5k} + \gamma_{5k} - \delta_{5k}.$$

In V-scheme, solutions of the equation system (12) have the form

$$r_2 = \frac{\Delta N}{D_V}\{\gamma_s[(\Gamma_m + \gamma_{42})(\Gamma_m + \gamma_{62}) - \delta_{42}\delta_{62}] -$$
$$-(\gamma_{42} - \delta_{62})[A^s_{42}(\Gamma_m + \gamma_{62}) + A^s_{62}\delta_{42}] - \tag{A.2}$$
$$-(\gamma_{62} - \delta_{42})[A^s_{62}(\Gamma_m + \gamma_{42}) + A^s_{42}\delta_{62}]\},$$

$$r_k = -\frac{\Delta N\Gamma_n}{D_V}[(\Gamma_m + \gamma_{l2})(\gamma_{k2} - \delta_{l2}) +$$
$$+(\gamma_{l2} - \delta_{k2})\delta_{l2}],$$

$$D_v = (\Gamma_n + \gamma_s)[(\Gamma_m + \gamma_{42})(\Gamma_m + \gamma_{62}) - \delta_{42}\delta_{62}] -$$
$$-(\gamma_{42} - \delta_{62})[A^s_{42}(\Gamma_m + \gamma_{62}) + A^s_{62}\delta_{42}] -$$
$$-(\gamma_{62} - \delta_{42})[A^s_{62}(\Gamma_m + \gamma_{42}) + A^s_{42}\delta_{62}],$$

$$A^s_{k2} = A_{k2} + \gamma_{k2} - \delta_{k2}, \quad k = 4,6, \quad l = 6,4,$$

$$\gamma_s = \gamma_{42} + \gamma_{62} - \delta_{42} - \delta_{62}.$$

APPENDIX B

In Λ-scheme, solutions of the equation system (17) for level population additions at $\Delta N_{5k} = \Delta N$ are as follows:

$$r_k = \frac{2\Delta N\Gamma_n}{D_\Lambda}\left[\frac{|G_{5k}|^2\,\Gamma_{mn}(\Gamma_m - A_{51} - A_{53})}{\Gamma^2_{mn} + \Omega^2_{5k}}\times\right.$$
$$\times\left(\frac{\Gamma_m - A_{5k}}{\Gamma_m - A_{51} - A_{53}} + \frac{2|G_{5l}|^2\,\Gamma_{mn}}{\Gamma_n(\Gamma^2_{mn} + \Omega^2_{5l})}\right) -$$
$$\left. - A_{5k}\frac{|G_{5l}|^2\,\Gamma_{mn}}{\Gamma^2_{mn} + \Omega^2_{5l}}\right],$$
$$k = 1,3, \quad l = 3,1,$$

$$r_5 = \frac{2\Delta N\Gamma^2_n}{D_\Lambda}\left[\sum_{1,3}\frac{|G_{5k}|^2\,\Gamma_{mn}}{\Gamma^2_{mn} + \Omega^2_{5k}} +\right.$$
$$\left. + \frac{2|G_{51}|^2\,\Gamma_{mn}}{\Gamma_n(\Gamma^2_{mn} + \Omega^2_{51})}\frac{2|G_{53}|^2\,\Gamma_{mn}}{\Gamma^2_{mn} + \Omega^2_{53}}\right], \tag{B.1}$$
$$D_\Lambda = \Gamma^2_n\Gamma_m\prod_{1,3}\left(1 + \frac{2|G_{5k}|^2\,\Gamma_{mn}}{\Gamma_n(\Gamma^2_{mn} + \Omega^2_{5k})}\right)\times$$
$$\times\left[1 + \sum_{1,3}\frac{\Gamma_n - A_{5k}}{\Gamma_m}\frac{2|G_{5k}|^2\,\Gamma_{mn}}{\Gamma_n[\Gamma^2_{mn}(1 + \frac{2|G_{5k}|^2}{\Gamma_{mn}\Gamma_n}) + \Omega^2_{5k}]}\right].$$

In V-scheme, solutions of the equation system (18) for level population additions at $\Delta N_{ik} = \Delta N$ have the form

$$r_2 = \frac{\Delta N}{D_V}\sum_{k=4,6}\frac{|G_{5k}|^2}{\Gamma_m}\frac{(\Gamma_m - A_{k2})\Gamma_{mn}}{\Gamma^2_{sk} + \Omega^2_{k2}},$$

$$D_V = \Gamma_n + \sum_{l=4,6}\frac{2|G_{l2}|^2}{\Gamma_m}\frac{(\Gamma_m - A_{l2})\Gamma_{mn}}{\Gamma^2_{sl} + \Omega^2_{l2}},$$

$$\Gamma^2_{sl} = \Gamma^2_{mn}(1 + \frac{2|G_{l2}|^2}{\Gamma_m\Gamma_{mn}}),$$

$$r_k = -\frac{\Lambda ND_V}{\Delta N}\frac{2|G_{5k}|^2}{\Gamma_m}\frac{\Gamma_{mn}}{\Gamma^2_{sk} + \Omega^2_{k2}}\times$$
$$\times\left[1 - \frac{\Gamma_m - A_{k2}}{D_V}\sum_{l=4,6}\frac{\Gamma^2_{mn}}{\Gamma^2_{sl} + \Omega^2_{l2}}\right],$$
$$k = 4,6. \tag{B.2}$$

REFERENCES

1. E. B. Aleksandrov, UFN **107**, 595 (1972).
2. W. E. Bell and A. L. Bloom, Phys. Rev. Lett. **6**, 280 (1961).
3. E. G. Saprykin, A. A. Chernenko, A.M. Shalagin, JETP **146**, 229 (2014).
4. G. Alzetta, A. Gozzini, L. Moi et al., Nouvo Cim. B **36**, 5 (1976).
5. E. Arrimondo and G. Orriols, Lett. Nouvo Cim. **17**, 333 (1976).
6. F. M. Akulshin, S. Barreiro, and A. Lesama, Phys. Rev. A **57**, 2996 (1998).
7. A. V. Taichenachev, A. M. Tumaikin, V. I. Yudin, JETP Lett. **69**, 776 (1999).
8. S. G. Rautian, JETP Lett. 60, 462 (1994).
9. S. K. Kim, H. S. Moon, K. Kim et al., Phys. Rev. A **61**, 063813 (2003).
10. D. V. Brazhnikov, A. V. Taichenachev, A. M. Tumaikin et al., JETP Letters **91**, 694 (2010).
11. C. Goren, A. D. Wilson-Gordon, M. Rosenbluh et al., Phys. Rev. A **67**, 033807 (2003).
12. D. V. Lazebnyi, D. V. Brazhnikov, A. V. Taichenachev et al., JETP **148**, 1068 (2015).
13. E. G. Saprykin, A. A. Chernenko, A. M. Shalagin, JETP **150**, 238 (2016).
14. S. G. Rautian, G. I. Smirnov, A. M. Shalagin, *Nonlinear Resonances in Atomic and Molecular Spectra*, Nauka, Novosibirsk (1979), p. 310.
15. A. M. Shalagin, *Fundamentals of High-Resolution Nonlinear Spectroscopy*, NSU, Novosibirsk (2008).
16. E. G. Saprykin, A. A. Chernenko, JETP **154**, 235 (2018).
17. E. G. Saprykin, A. A. Chernenko, QE **49**, 479 (2019).
18. E. G. Saprykin, A. A. Chernenko, QE **52**, 560 (2022).
19. A. Chernenko and E. Saprykin, Amer. J. Opt. Phot. **8**, 51 (2020).
20. V. S. Letokhov, V. P. Chebotaev, *Principles of Nonlinear Laser Spectroscopy,* Nauka, Moscow (1975), p. 512.
21. E. G. Saprykin, A. A. Chernenko, Opt. Spectrosc. **127**, 671 (2019).